EFFECT OF CARBONIZATION CONDITIONS OF POLYANILINE ON ITS CATALYTIC ACTIVITY TOWARDS ORR. SOME INSIGHTS ABOUT THE NATURE OF THE ACTIVE SITES

Javier Quílez-Bermejo[1], Carolina González-Gaitán[2], Emilia Morallón[2], Diego Cazorla-Amorós[1]

[1]Departamento de Química Inorgánica and Instituto de Materiales. Universidad de Alicante, Ap. 99, 03080, Alicante, Spain

[2]Departamento de Química Física and Instituto de Materiales. Universidad de Alicante, Ap. 99, 03080, Alicante, Spain

ABSTRACT

N-doped carbon materials were obtained using polyaniline (PANI) as precursor. Heat treatment of PANI and de-doped PANI (PANId) was performed using different temperatures – 600 and 800 ºC –. Two different atmospheres were used during the treatment: an inert atmosphere (N_2) and another one consisting on a slightly oxidizing mixture of gases (3000 ppm O_2 in N_2). The prepared materials at 800 ºC showed high values of capacitance, up to 170 and 255 F g^{-1} in basic and acid electrolytes, respectively, in spite of their low surface area. The electrocatalytic activity towards oxygen reduction reaction (ORR) of all materials was studied in basic and acid media. The heat treated materials at 600 ºC did not show a good electrocatalytic activity due to their poor electrical conductivity. On the other hand, heat-treated materials at 800 ºC showed an enhanced catalytic activity due to their higher conductivity and the presence of nitrogen and oxygen functionalities in the carbon surface. Interestingly, the heat treatment at 800 ºC using a slightly oxidant atmosphere produces carbon materials with much higher ORR activity which seems to be related to the larger amount of N-edge and O-edge sites. Preliminary computational studies suggest that the presence of these nitrogen and oxygen functionalities in the vicinities of the carbon atom improves the catalytic performance of N-doped carbon materials in the ORR and that two adjacent active sites can produce the O_2 reduction to H_2O through a 4 electrons pathway.

1. INTRODUCTION

The oxygen reduction reaction (ORR) occurring in the cathode of the fuel cells is a key factor in the development and commercialization of these devices [1]. This reaction is a limiting factor of the fuel cells due to its slow kinetics and high overpotential, which makes necessary the use of high efficient catalysts for its practical use [2]. The most commonly used electrocatalysts are based on platinum as active phase supported on different carbon materials [3–7]. So far, these catalysts show the best activities; however, their high cost, low availability of the metal in nature, the vulnerability to poisoning and electrochemical deactivation, affect their efficiency and useful life [8,9]. Therefore, it is necessary to develop new catalysts for the ORR with higher efficiencies for their use in fuel cells.

Nowadays, significant scientific efforts focus on the development of new non-noble metal catalysts. There are two different approaches in order to replace Pt and other noble metals. One is the use of non-noble metals – usually transition metals as Co, Ni, Fe –, which have a higher availability and lower costs [10]. The second and more innovative alternative is the development of metal-free catalysts based on carbon materials doped with different heteroatoms [11,12]. In this sense, nitrogen-doped carbon materials are one of the most promising materials due to their high activity and stability at the working conditions [13]. The effect of nitrogen is still under study; some authors suggest that the presence of nitrogen changes the geometry and the electron-donor character of the material, which affects the acidity/basicity of the carbon material [14,15]. It causes a redistribution of the electronic density in the vicinity of the heteroatoms and the nitrogen atoms induce a positive charge in the carbon atom located in the vicinities, which promotes the chemisorption of oxygen and weakens the oxygen-oxygen bond [16–18].

Nitrogen-doped carbon materials can be synthesized by several methods [13,19–22]: (i) thermal decomposition of a nitrogen-containing precursor or polymer in the presence of the carbon material, (ii) reaction of a carbon material with a nitrogen-containing reagent, (e.g. ammonia, urea, NO), (iii) carbonization or chemical vapor deposition, followed or not by a chemical or

physical activation of a nitrogen-containing precursor and (iv) hydrothermal carbonization of nitrogen-containing biomass precursors. The first of these methods comprises the use of different polymers with a high nitrogen content. Polypyrrole (PPy) and polyaniline (PANI) are good alternatives for this use and several studies have shown that their carbonization leads to materials with a high nitrogen content and other properties, which are promising for electrocatalysis and energy storage applications [22,23].

Heat treatment at different temperatures of PPy and PANI has been analyzed in inert or reducing atmosphere generating a carbon material with a good ORR activity [24]. However, to the best of our knowledge the use of an oxidant-containing atmosphere has not yet been studied. In this sense, this work presents the preparation of nitrogen-doped carbon materials synthesized by heat treatment of PANI at different temperatures using inert or a slightly oxidant atmosphere during the treatment. The electrochemical behavior and the physicochemical properties of the prepared materials were determined and their electrocatalytic activity towards ORR in alkaline and acid media has been assessed. The use of the slightly oxidizing atmosphere produces materials with the highest ORR activity, which is a consequence of the changes in surface chemistry induced by this treatment. A detailed analysis of the surface chemistry of the prepared materials allows to propose some insights about the nature of the active sites for this reaction.

2. EXPERIMENTAL

2.1 Materials and reagents

Aniline was purchased from Sigma Aldrich and was distilled by refluxing under reduced pressure prior its use in order to remove the impurities (e.g. aniline oligomers formed by oxidation during the storage). Ammonium persulfate ($(NH_4)_2(S_2O_8)$), ammonium hydroxide (NH_4OH), potassium hydroxide (KOH), polytetrafluoroethylene (60% PTFE) and Pt/Vulcan (20% loading) were purchased from Sigma-Aldrich. Hydrochloric acid (37 % HCl) and perchloric acid (60%, $HClO_4$) were purchased from VWR-Chemicals Prolabo. All the solutions were prepared using ultrapure water (18 $M\Omega$ cm from an Elga Labwater Purelab system). The

gases N_2 (99.999%), O_2 (99.995%), H_2 (99.999%) and synthetic air were provided by Air Liquide and were used without any further purification or treatment.

2.2 PANI preparation

PANI was prepared by chemical polymerization from a solution of 1 M HCl containing 0.67 M of aniline and ammonium persulfate in a stoichiometric ratio [22]. The mixture was kept under stirring (500 rpm) for 2 h at 0 ºC. In order to obtain the de-doped PANI (PANId), after the 2 h of polymerization process, 3.4 g of the obtained PANI was treated with 1 M NH_4OH for 24 h. The synthesized PANI and PANId were washed several times with distilled water and dried at 120 ºC overnight.

2.3 Heat treatment

The samples (150 mg of PANI or PANId) were heat treated in a tubular furnace at 600 and 800 ºC for 1 h using a heating rate of 5 ºC min^{-1}. Two different atmospheres were used for the treatment: an inert (N_2) and a slightly oxidant atmospheres (3000 ppm O_2 in N_2). The furnace was purged for 1 h before the heat treatment in the corresponding atmosphere, the flow rate was maintained at 100 ml min^{-1} during the treatment. The samples are referred as PANI_X_Y and PANId_X_Y for the as synthesized PANI and de-doped PANI, respectively, being X the atmosphere and Y the carbonization temperature used during the heat treatment.

2.4 *Physicochemical characterization*

The textural properties of the materials have been evaluated by N_2 adsorption isotherms at -196 °C and CO_2 adsorption at 0ºC in an automatic adsorption system (Autosorb-6, Quantachrome). Prior to the measurements, the samples were degassed at 250 °C for 4 h. Apparent surface areas have been determined by BET method (S_{BET}) and total micropore volume (pores of size < 2 nm) has been assessed by applying Dubinin-Radushkevich (DR) equation to the N_2 adsorption isotherms. The narrow micropore volume (pores of size < 0.7 nm) was calculated from CO_2 adsorption isotherms at 0 ºC using DR equation [25].

The samples were characterized by Transmission Electron Microscopy (TEM) coupled to EDX with a JEOL JEM-2010 microscope operating at 200 kV with a spatial resolution of 0.24 nm. Raman spectra were collected on a Jasco NRS-5100 spectrometer. A 3.9 mW He–Ne laser at 633 nm was used. The spectra were acquired for 120 s. The detector was a Peltier cooled charge-coupled device (CCD) (1024 × 255 pixels). Calibration of the spectrometer was performed with a Si slice (521 ± 2 cm^{-1}).

The surface composition and oxidation states of the elements of the prepared materials were studied using XPS in a VG-Microtech Mutilab 3000 spectrometer with an Al Kα radiation source (1253.6 eV). The deconvolution of the N1s XPS spectra was done by least squares fitting using Gaussian-Lorentzian curves, while a Shirley line was used for the background determination. Elemental analysis of the materials was performed in an Elemental CHNS Microanalyzer with Micro TruSpec detection system from LECO.

In order to check the role of the oxygen during the heat treatment, PANId sample was subjected to thermogravimetric analysis in different conditions using a thermobalance (SDT 2960 instrument, TA). Heat treatment of PANId was performed in air at 250 ºC until the weight was stable (1 h 15 min), then the atmosphere was changed to N_2 and heated up at 800 ºC for 30 min (heating rate of 5 ºC min^{-1}). Heat treatment in N_2 was also performed in a different sample for comparison purposes.

Temperature programmed desorption (TPD) experiments were performed in a DSC-TGA equipment (TA Instruments, SDT 2960 Simultaneous) coupled to a mass spectrometer (Thermostar, Balzers, GSD 300 T3) which was used to follow the m/z lines related to the decomposition of surface functional groups from the surface of the carbon materials. The thermobalance was purged for 2 hours under a helium flow rate of 100 ml min^{-1} and then heated up to 950°C (heating rate 20°C min^{-1}).

2.5 Electrochemical measurements

The electrochemical characterization of the materials was performed in a Biologic VSP potentiostat using a standard three-electrode cell configuration, with a platinum wire as counter electrode and Ag/AgCl electrode as reference electrode. However, all potentials will be referred to the reversible hydrogen electrode (RHE).

The electrochemical behavior was studied by cyclic voltammetry (CV) in 0.1 M KOH and 0.1 M $HClO_4$ between 0.0 and 0.8 V (vs. RHE). The working electrode was prepared by mixing the carbon material with acetylene black as a conductive promoter and PTFE as binder in a proportion 90:5:5, respectively. A disk molded of the dry paste containing ~ 15 mg and 1 cm^2 was placed in a stainless steel mesh and pressed for 5 min at 2 tons to guarantee a homogeneous thickness.

The study of the electrocatalytic activity towards ORR was performed in an Autolab PGSTAT302 (Metrohm, Netherlands) potentiostat. A rotating ring-disk electrode (RRDE, Pine Research Instruments, USA) equipped with a glassy carbon disk (5.61 mm diameter) and an attached platinum ring was used as the working electrode, a platinum wire as the counter electrode and a reversible hydrogen electrode (RHE) immersed in the working electrolyte as the reference electrode. The amount of catalyst on the disk electrode was optimized in order to reach the highest limiting current, being 120 μg the optimum value. Therefore, the glassy carbon disk was modified with the samples using 120 μl of a 1 mg ml^{-1} dispersion of each carbon material (20% isopropanol, 0.02% Nafion®), obtaining a catalyst loading of 0.48 mg cm^{-2}.

The electrocatalytic activity towards ORR was studied by linear sweep voltammetry (LSV) in O_2 saturated 0.1 M KOH and 0.1 M $HClO_4$ between 0.0 and 1.0 V (vs. RHE) at different rotation rates, from 400 to 2025 rpm and at a scan rate of 5 mV s^{-1}. The potential of the ring was held constant at 1.5 V (vs. RHE) during all measurements. The onset potential was measured at a current density of -0.3 mA cm^{-2} for all samples. The electron transfer number was calculated from the hydrogen peroxide oxidation in the Pt ring electrode as follows:

6

$$n = \frac{4\,I_d}{I_d + I_r/N}$$ **Eq. 1**

Where I_r and I_d are the current measured at the ring and the disk, respectively, and N is the collection efficiency of the ring, which was experimentally determined to be 0.37.

In order to study the stability of the catalysts, chronoamperometric experiments were performed. The disk was held at a potential of 0.57 V (vs. RHE) using a rotation rate of 1600 rpm. The tests lasted for 15 hours, and the current in the disk was tracked during the experiment.

2.6 Computational calculations

Initial representative structures of the proposed active sites were drawn in Avogadro Version 2.0.8.0 [26], which was also used for the geometrical optimization. The determination of the electronic density was performed with Gaussian 09 using density functional theory (DFT) with b3lyp/6-31 g(d) level of approximation [27].

3. RESULTS AND DISCUSSION

3.1 Materials preparation

The carbonization yields obtained after the heat treatment performed to the PANI and PANId are presented in Table 1. The values for the materials prepared from PANId are slightly higher independently of the temperature and atmosphere used during the heat treatment. These differences can be attributed to the loss of the Cl⁻ counter ion in the PANI-based samples. Additionally, the use of an inert atmosphere also renders a lower yield (around 10 wt% lower), indicating that the presence of oxygen promotes the crosslinking reactions between the polymer chains, which favor the condensation reactions during the carbonization. These crosslinking reactions are well-known in stabilization processes of different carbon materials (for example those used for carbon fiber preparation) that occur at low temperatures due to oxygen chemisorption [28]. It is important to note that, for the sample mass/gas flow ratio employed in this study and the low O_2 concentration used, most of the O_2 is used in the stabilization reactions occurring in the pristine polymer (in agreement with the observed higher yields) and in the

oxidation of the decomposition molecules formed during the carbonization, which have a higher reactivity than the remaining carbon material.

Table 1 Carbonization yields and porous texture characterization results for all materials

Sample	Yield / wt%	S_{BET} / $m^2\ g^{-1}$	V_{DR} (N_2) / $cm^3\ g^{-1}$	V_{DR} (CO_2) / $cm^3\ g^{-1}$
PANI_N2_600	57	384	0.16	0.16
PANId_N2_600	68	340	0.14	0.14
PANI_O2_600	60	403	0.17	0.16
PANId_O2_600	76	394	0.16	0.13
PANI_N2_800	47	530	0.20	0.24
PANId_N2_800	58	526	0.20	0.24
PANI_O2_800	58	628	0.24	0.26
PANId_O2_800	71	584	0.22	0.24

To check the relevance of the crosslinking reactions occurring at low temperatures, the carbonization of PANId sample was studied by TG, with or without any stabilization treatment in O_2. The results in Fig. 1 show that the heat treatment in N_2 up to 800ºC produces a yield of around 46 wt% (blue line in Fig. 1), whereas a previous heat treatment in air at 250ºC results in a final yield around 66 wt% (red line in Fig. 1), being these values in agreement with the final yields obtained in the tubular furnace (Table 1).
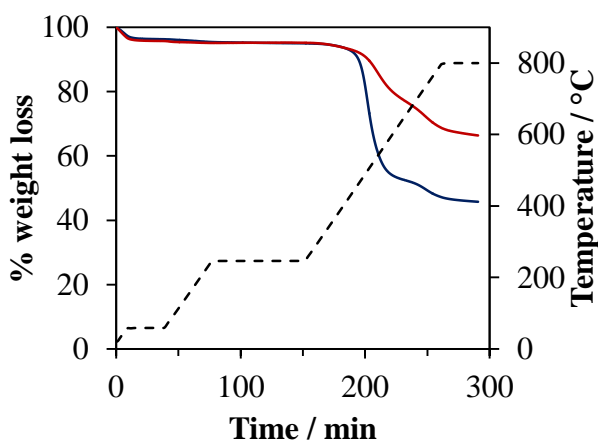

Fig. 1 TG profiles of PANId treated in air at 250ºC and then heated up at 800ºC in N_2 atmosphere (red line) and PANId treated at in N2 at 800ºC (blue line). Dashed line shows the temperature profile during the treatment.

3.2 Physicochemical characterization

Fig. 2 shows the N_2 adsorption isotherms for all materials and Table 1 summarizes the porous texture data. All materials present type I isotherms, characteristic of microporous materials. The BET surface areas calculated for all materials show that a heat treatment at 800 ºC results in a higher surface area independently of the atmosphere used. The treatment in an oxidant atmosphere only leads to materials with a somewhat higher surface area when the PANI sample is heated at 800ºC, that can be related with the more complex carbonization process that includes the evolution of Cl^- anions probably as HCl molecules. The micropore volumes calculated from N_2 and CO_2 are similar for each sample, indicating that they all have similar pore size distribution consisting of a homogeneous narrow microporosity of size around 0.7 nm [25].
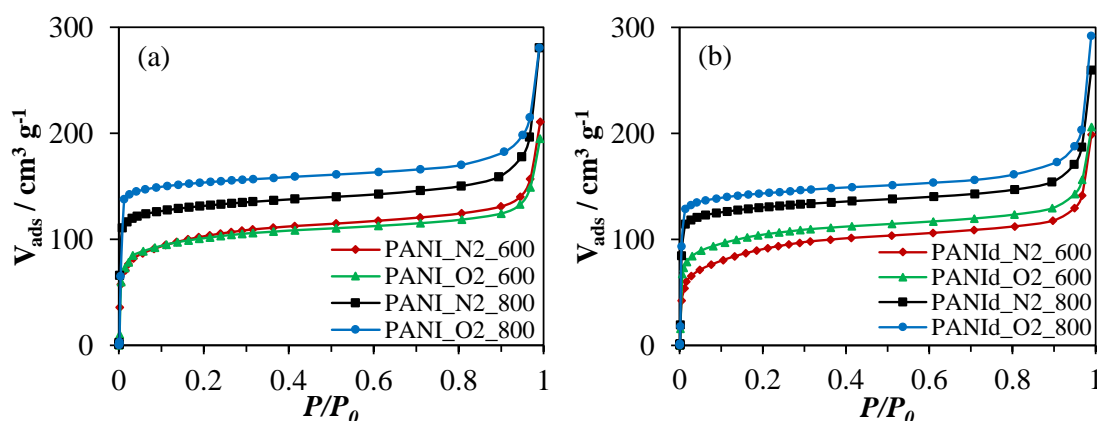

Fig. 2 N_2 adsorption isotherms at -196 °C of the materials prepared at (a) 600 ºC and (b) 800 ºC

The morphology of the prepared materials was characterized by transmission electron microscopy (TEM). The images (Fig. S1) show a similar laminar morphology for all samples and only small differences are observed for the sample treated in O_2-containing atmosphere at 800ºC. It seems that this sample presents a higher roughness at the borders, suggesting a different chemical structure in this region, which is related to the use of slightly oxidant atmosphere during the heat treatment. Raman spectroscopy was used for structural characterization of the materials. Raman spectra (Fig. S2) reveal the D and G bands, characteristic of graphene based carbons. The spectra are similar for all samples.

Table 2 presents the bulk elemental composition of all materials obtained by elemental analysis using a CHNS Microanalyzer. PANI and PANId present differences in their elemental composition. The main difference is the lower amount of carbon in PANI sample and a high oxygen content calculated by difference, which includes the O and Cl content in this sample. The carbon content of the materials treated in a N_2 atmosphere is always higher than the samples treated in the O_2-containing atmosphere at the corresponding temperature. Furthermore, the nitrogen content for the samples treated at 600 °C are similar between them independently of the atmosphere used during the heat treatment. On the other hand, when the heat treatment is performed in an O_2-containing atmosphere at 800 °C, the nitrogen content slightly increases. In general, all materials have a high nitrogen content, from 6.6 to 12.7 wt%.

Table 2 Elemental composition of the materials obtained by elemental analysis

Sample	C / wt %	N / wt %	H / wt %	O / wt % *
PANI	57.8	12.4	4.9	24.9[**]
PANId	74.5	15.2	4.6	5.7
PANI_N2_600	76.2	12.1	2.7	9.0
PANId_N2_600	76.6	12.4	2.8	8.2
PANI_O2_600	73.7	12.0	1.9	12.4
PANId_O2_600	75.6	12.7	2.2	9.5
PANI_N2_800	80.2	6.6	1.4	11.8
PANId_N2_800	80.3	7.0	1.4	11.3
PANI_O2_800	76.1	7.4	1.4	15.1
PANId_O2_800	76.9	7.6	1.3	14.2

*Oxygen content was calculated by difference
**This value includes the O and Cl content

The chemical nature of the N functionalities has been studied by XPS. N1s spectra for all materials show differences in the type of nitrogen species present in the samples depending on the temperature used in the heat treatment (Fig. 3). After a heat treatment at 600 ºC, two different contributions can be distinguished, at around 398.5 and 400.3 eV, associated to the presence of pyridine and pyrrole and/or pyridone groups, respectively [29–31]. On the other hand, when the heat treatment is performed at 800 ºC, a new peak appears above 401 eV, assigned to quaternary nitrogen [30], which is in agreement with previous results [31] and with the PANI carbonization mechanism reported in the literature [32,33]. Starting at 400 ºC, the

breaking of bonds and cross-linking reactions occur [33] and up to 600 ºC the reconstruction of the backbone of the polymer takes place [32]. The initial amino groups of the aniline form pyridine and pyrrole species. The heat treatment up to 800 ºC results in condensation reactions where quaternary nitrogen species are formed and the amount of pyrrole groups decreases. It seems that the differences among both atmospheres in XPS peak position are minor except for a small shift of BE to higher values in some cases when O_2 is used in the carbonization atmosphere, what can be related to the higher oxygen content of these samples.
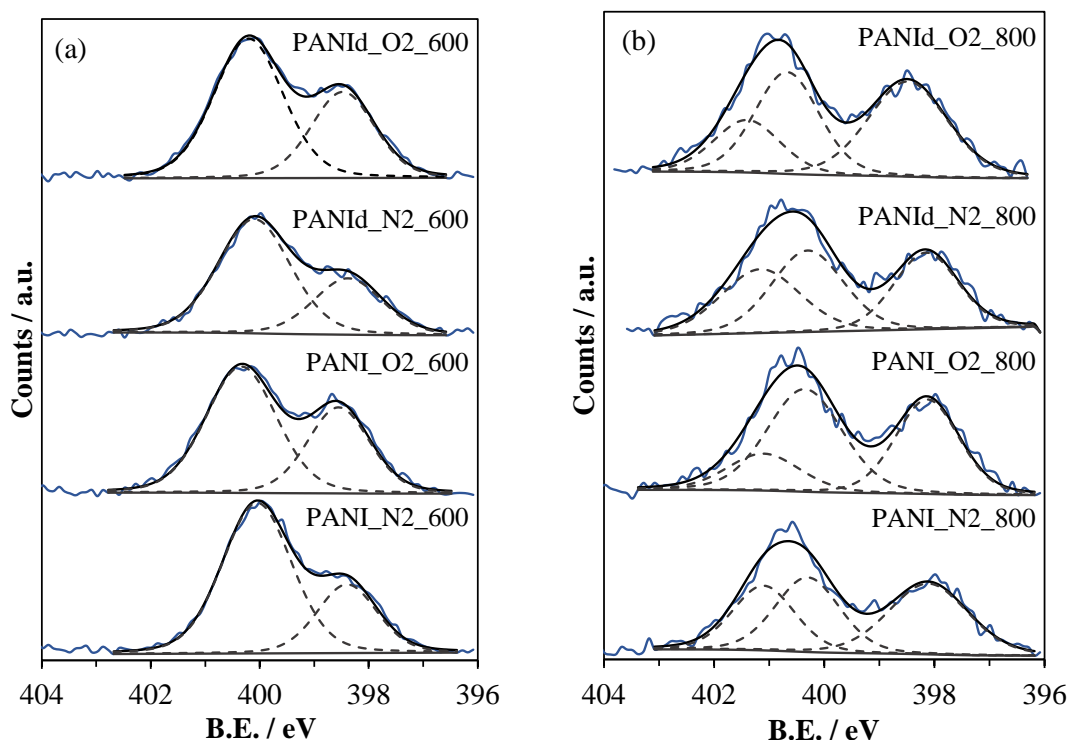
Fig. 3 N1s spectra of the materials prepared at (a) 600 ºC and (b) 800 ºC

However, if we observe the percentage of each N-species obtained from the XPS deconvolution (Table 3), some interesting aspects should be emphasized. Firstly, there are no significant differences between the samples prepared at 600 ºC. However, a heat treatment at 800 ºC produces differences depending on the atmosphere used during the heat treatment. The use of a slightly oxidant atmosphere produces a higher contribution of pyridine and pyrrole/pyridone-like nitrogen species and a lower amount of quaternary nitrogen. This means that the use of an

11

O$_2$-containing atmosphere produces a higher concentration of N-species at edge sites and less at basal planes, what is an interesting observation.

Table 3 Percentage of each nitrogen group for all materials

Sample	% Pyridine	% Pyrrole/Pyridone	% Quaternary nitrogen
PANI_N2_600	32	68	--
PANId_N2_600	34	66	--
PANI_O2_600	39	61	--
PANId_O2_600	36	64	--
PANI_N2_800	39	33	28
PANId_N2_800	31	37	32
PANI_O2_800	37	47	17
PANId_O2_800	43	37	20

The surface chemistry related to oxygen functional groups was studied by temperature-programmed desorption (TPD). The decomposition of surface oxygen functionalities using TPD is a well-known process that has been extensively used for characterizing the surface functionalities of carbon materials [34–39]. CO evolution is related to the decomposition of neutral and basic groups such as carbonyl, quinones, phenols and ethers, which evolve as CO at different temperatures. Likewise, CO$_2$ desorption is primarily related to the decomposition of acid groups as carboxylic, anhydride and lactone groups [34–39]. For these materials, CO$_2$ desorption (not included) does not show significant differences among both treatments. However, the CO profile reveals important changes. Fig. 4 shows the CO-TPD profiles for PANId_N2_800 and PANId_O2_800. In both samples, the CO profile has a peak at around 750 ºC related to the presence of phenolic groups [34]. However, this peak has higher intensity for the PANId_O2_800 sample, which points out that the O$_2$-containing atmosphere promotes the formation of these kind of species.

This means that the samples heat treated in the O$_2$-containing atmosphere at 800ºC contain a larger concentration of pyridine, pyridone/pyrrole N functionalities and a higher amount of phenol-like oxygen groups, being all of them at edge sites.
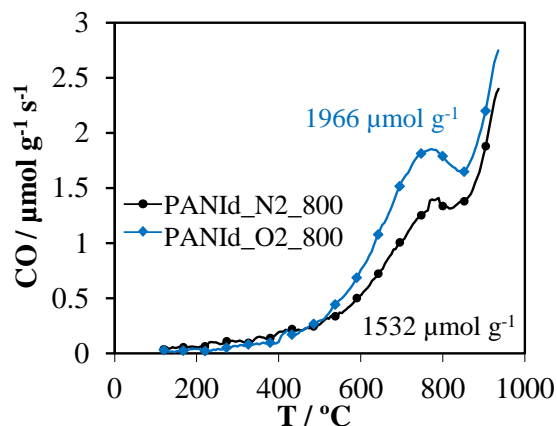
Fig. 4 CO-TPD profiles for PANId_N2_800 and PANI_O2_800.

3.3 *Electrochemical characterization*

Fig. 5 shows the cyclic voltammograms of the samples heat treated at 800 °C in 0.1 M KOH and 0.1 M HClO₄, respectively. In basic medium, all samples show a trapezoidal shape with a high electrical double layer charge, being higher for the samples treated in an O_2-containing atmosphere. They have the characteristic shape observed for N-doped carbon materials in alkaline electrolytes [40]. On the other hand, voltammograms in acid medium show a quasi-rectangular shape for all materials. No significant differences are seen for the samples prepared from PANI and PANId as a precursor after applying the same heat treatment, which is expected due to their similar structures and chemical composition.
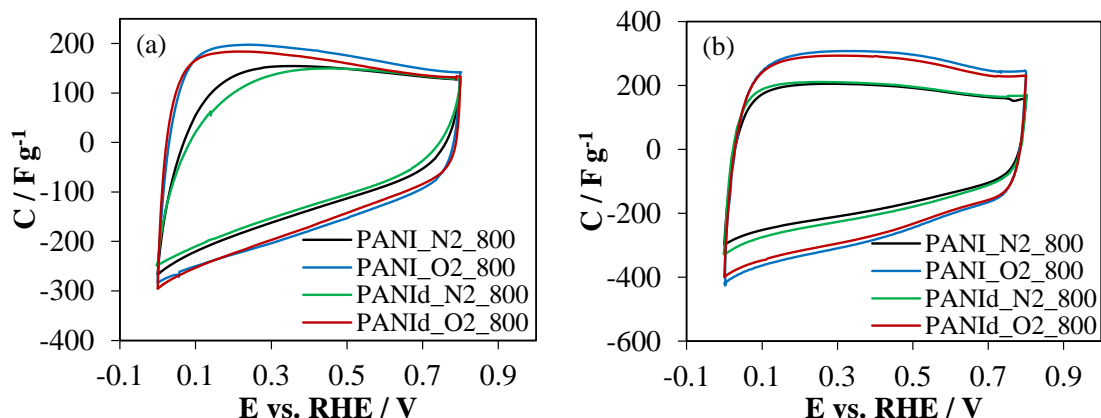

Fig. 5 Steady state voltammograms for the different materials prepared at 800 °C in (a) 0.1 M KOH and (b) 0.1 M HClO₄. v = 1 mV s^{-1}.

13

Table 5 includes the gravimetric capacitance values obtained from the cyclic voltammetry experiments showed in Fig. 5 for the samples treated at 800 °C in the two electrolytes. All samples treated at 800 °C present high capacitance values up to 170 and 255 F g^{-1} in alkaline and acid electrolyte, respectively. These high values are in agreement with others reported in literature for N-doped carbon materials, which proposed that nitrogen groups are electrochemically active or favor wettability, resulting in significantly enhanced capacitance in aqueous electrolytes [41,42]. The lower capacitance values obtained for the samples treated in N_2 can be due to the differences in surface chemistry or to slight differences in porosity that can have an important influence in electrolyte accessibility (Table 1).

Table 5 Gravimetric capacitance of the samples

Sample	Capacitance / F g^{-1}	
	0.1 M KOH	0.1 M HClO$_4$
PANI_N2_800	107	180
PANId_N2_800	100	191
PANI_O2_800	170	254
PANId_O2_800	162	255

3.4 Electrocatalytic activity towards ORR

The electrocatalytic activities towards ORR of all materials were studied in O_2-saturated 0.1 M KOH and 0.1 M HClO$_4$ solutions. Linear sweep voltammetry analysis was performed using a RRDE at different rotation rates. The current registered in the Pt ring electrode is related to the amount of H_2O_2 formed in the disk electrode during the ORR, which is the intermediate compound found in the 2 e^- pathway. Fig. 6 shows the LSV curves at 1600 rpm for all samples in 0.1 M KOH electrolyte. The LSV for commercial 20% Pt/Vulcan has been included for comparison purposes. Fig. 6c shows, as an example, the LSV curves for the sample PANId_O2_800 at different rotation rates, the behavior is similar for all tested samples. Table 6 presents the most relevant ORR kinetic parameters derived from the RRDE measurements.

In alkaline medium, the samples treated at 600 ºC show a poor performance (Fig 6a), being closer to the bare glassy carbon electrode, pointing out their low ORR activity. It can be attributed mainly to the low electrical conductivity of the materials due to the low temperature used during the treatment. On the other hand, there are no significant differences when PANI or PANId are used as precursor materials indicating that the Cl⁻ counter ion is removed during the heat treatment leaving no substantial changes in the final materials, and therefore in their catalytic activity.

Interestingly, significant differences are observed for samples heat-treated at 800 ºC depending on the atmosphere used during the heat treatment (Fig. 6b). The samples treated in a slightly oxidant atmosphere show both higher onset potential values and limiting current densities, reaching in this last parameter values close to that for the commercial 20% Pt/Vulcan sample. These results could be associated to the different nitrogen and oxygen functionalities in the carbon surface. According to elemental analysis and TPD results, samples treated in inert atmosphere have lower nitrogen and oxygen contents than the samples treated in a slightly oxidant atmosphere. Additionally, the XPS showed that the use of a slightly oxidant atmosphere leads to the formation of a higher amount of N functionalities at edge sites, which have been suggested to play a role in the electrocatalytic performance to the ORR [11,14,43,44]. In addition, a larger concentration of phenol-type functional groups observed by TPD, indicates that a higher amount of both N and O functional groups at edge sites exists for the sample treated in the O_2-containing atmosphere. The results suggest that the larger amount of N-edge and O-edge sites is related to the higher activity towards ORR observed for these samples. These heteroatoms may form N-C-O species, which can be sites with higher activity in agreement with the literature [45].
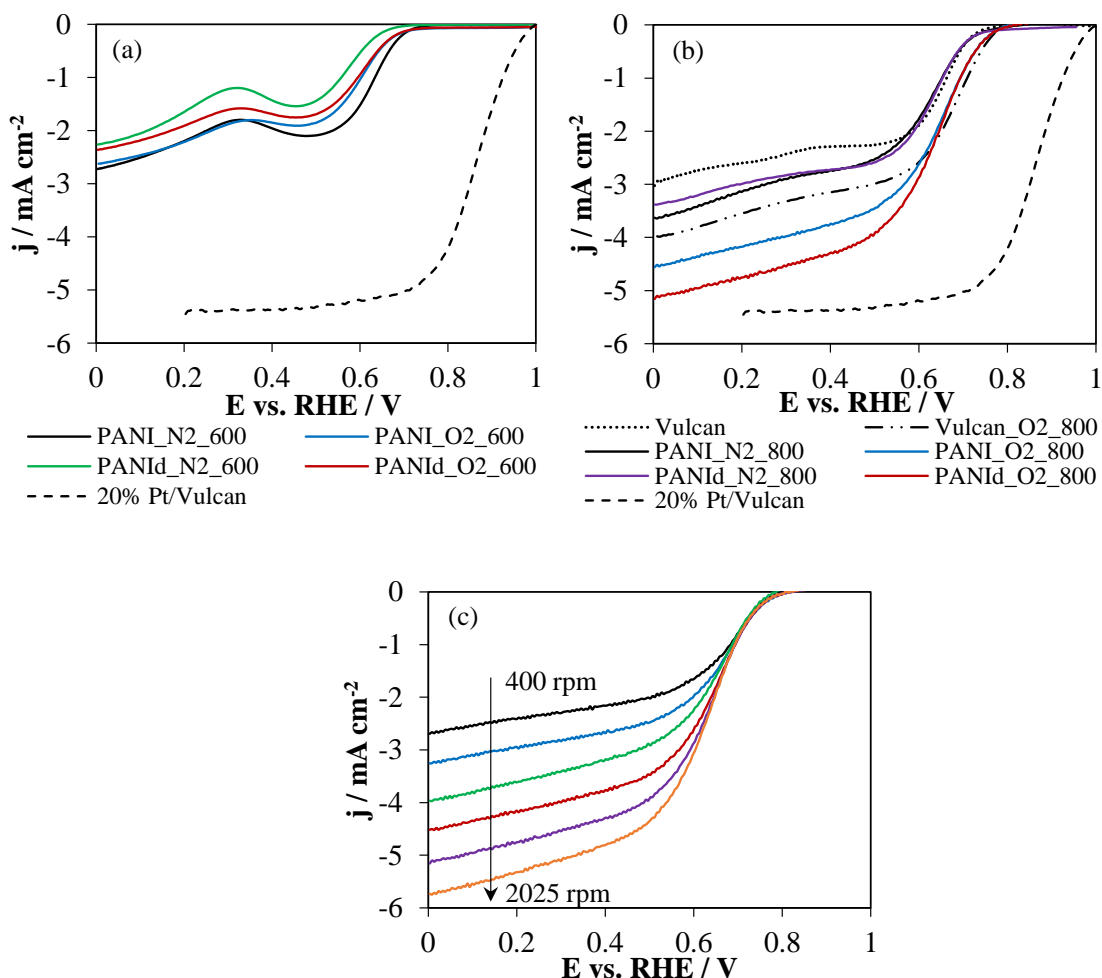
Fig. 6 (a), and (b) Linear sweep voltammetry curves for the prepared materials in O_2-saturated 0.1 M KOH at 5 mV s^{-1} and 1600rpm. (c) Linear sweep voltammetry curves of PANId_O2_800 electrode in O_2-saturated 0.1 M KOH at 5 mV s^{-1} at different rotation rates.

In order to confirm the beneficial use of a slightly oxidant atmosphere, Vulcan sample was also tested as electrocatalyst towards ORR. The same treatment at 800 ºC in the oxidant atmosphere was performed for this material. Fig. 6b shows the LSV curve for this sample, and pristine Vulcan is also included for comparison purposes. It is possible to see that the heat treatment using the oxidant atmosphere improves the catalytic activity of the pristine Vulcan, with an onset potential close to the obtained for PANI_O2_800 and PANId_O2_800 but with a lower current density. However, non-treated Vulcan has a performance similar to the PANI samples treated in N_2. This means that the surface oxygen functionalities generated during the treatment increase the ORR activity. However, the higher ORR activity found for the PANI samples

treated in an O_2-containing atmosphere <mark>suggests</mark> that the carbon atom sites with neighbor nitrogen and oxygen functionalities have an enhanced ORR activity.

Table 6 Electrochemical parameters calculated from the RRDE experiments of the different electrocatalysts in O_2-saturated 0.1 M KOH and 0.1 M $HClO_4$ at 5 mV s^{-1} and 1600 rpm.

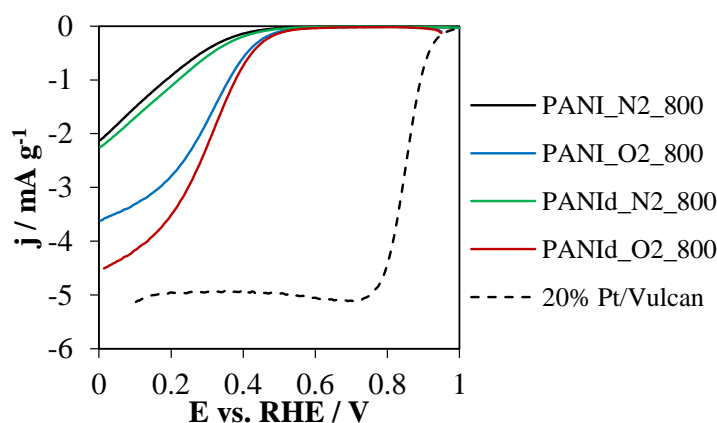| Sample	0.1 M KOH		0.1 M HClO₄	
	E_{onset} vs. RHE / V	n at 0.3 V	E_{onset} vs. RHE / V	n at 0.1 V
PANI_N2_600	0.68	2.2	--	--
PANId_N2_600	0.63	2.2	--	--
PANI_O2_600	0.72	2.6	--	--
PANId_O2_600	0.71	2.3	--	--
PANI_N2_800	0.66	2.6	0.22	3.4
PANId_N2_800	0.66	2.5	0.35	3.2
PANI_O2_800	0.75	2.8	0.46	3.8
PANId_O2_800	0.75	3.0	0.46	3.8
Vulcan	0.71	2.2	--	--
Vulcan_O2_800	0.75	2.5	--	--
20% Pt/Vulcan	0.94	3.9	0.93	4.0

Fig. 7 Linear sweep voltammetry curves of the prepared materials in O_2-saturated 0.1 M $HClO_4$ at 5 mV s^{-1} and 1600rpm.

Fig. 7 includes the LSV curves in 0.1 M $HClO_4$ solution for the samples treated at 800 ºC since they showed the best performance towards ORR in alkaline medium. As expected, the samples treated in a slightly oxidant atmosphere show an enhanced ORR activity compared to the prepared using N_2 atmosphere. The onset potential and current density are far from the obtained for the commercial Pt/Vulcan sample, although slightly higher current densities than the previously reported in the literature have been obtained [11,46].

The electron transfer number obtained during the ORR was followed by the current registered in the Pt ring during the experiments. Table 6 presents the values at 0.3 V for all materials in alkaline medium. Interestingly, samples PANI_O2_800 and PANId_O2_800 show an electron transfer number close to 3, which could be related to a combined mechanism of a 2 and 4 e$^-$ pathway or a 2 + 2 e$^-$ pathway. The former is related to the possibility of having two different active sites and the latter to a first 2 e$^-$ reduction to hydroperoxide, and a second 2 e$^-$ reduction of the hydroperoxide intermediate to water, which can occur during the diffusion of the molecules inside the porosity of the carbon material [47,48]. In acid medium, in spite of the much lower activity, the 4 e$^-$ mechanism is favorable for the samples treated in an O_2-containing atmosphere (Table 6).

3.5 Stability of the catalyst

The stability of PANId_O2_800 was evaluated under potentiostatic conditions since it was the catalyst that showed the best electroactivity towards ORR. Fig. 8 shows the current versus time plots for PANId_O2_800 and 20% Pt/Vulcan catalysts. The experiments were performed in 0.1 M KOH at a potential of 0.57 V in which the limiting specific current was reached for these catalysts. The results show a 20% loss in the current for PANId_O2_800 after 15 hours. An initial decrease is observed during the first 3 hours and, after that, the activity of the catalyst remains constant. In contrast, the decrease in activity for the Pt-based catalyst is 38% after the same testing time, pointing out the good stability of prepared material looking forward practical applications.
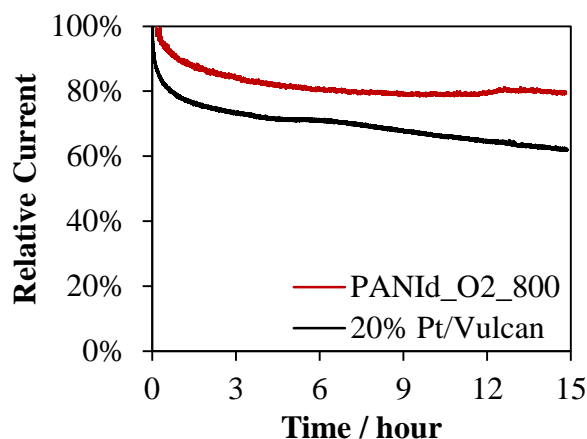
3.6 Computational study

In order to examine the possible active sites present in the catalysts, calculations of the electronic density were performed for different simple model structures. According to the experimental results, it seems that the carbon atoms in N-C-O species may constitute the active sites with the highest activity for the ORR. Fig. 9 shows the model structure of different possible actives sites that could be present in the prepared materials. The <mark>effective charge</mark> of each atom is also plotted for the different <mark>model</mark> structures. Fig. 9a includes a pyridone group; the calculation of the electronic density of the molecule allows us to confirm that the carbon atom between the nitrogen and oxygen atoms has the largest positive charge value, being the site where the dioxygen molecule would be adsorbed and then reduced. Fig. 9b includes two consecutive pyridone groups in which the two carbon atoms bonded to N and O, have a charge similar to the structure with only one pyridone (Fig. 9a). Finally, Fig. 9c corresponds to a structure containing two pyridine functional groups. In this case, the neighbor carbon atoms have a smaller change in electronic density compared to the structures with the –OH functional groups. This suggests that the ORR activity will be higher for the carbon atoms with nitrogen and oxygen heteroatoms in its vicinities, which is in agreement with the experimental results. The low activity of pyridine like species has already been proposed in the literature [49].<mark>The effective charge of the adjacent C atom in an N-C-O type group (0.452) is considerable higher</mark>
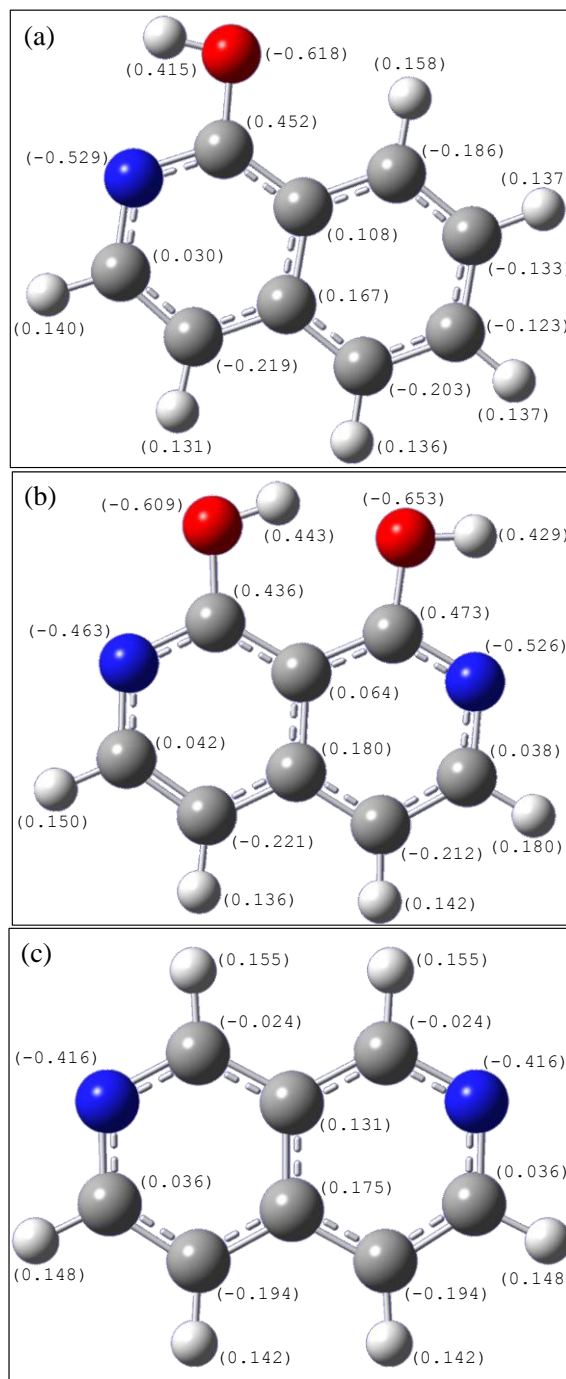
19

Fig. 9 Model structures for different heteroatom-containing molecules and the calculated effective charge of all atoms: (a) one pyridone group, (b) two adjacent pyridones groups and (c) pyridine. H is white, C is grey, N is blue, and O is red.

From the previous model structures, we propose two different possible reaction pathways for the ORR, which are shown in Fig. 10. The first one (Fig 10a) starts with the presence of one N-C-O active site (model structure shown in Figs. 9a and b), in which the dioxygen molecule is adsorbed forming the intermediate –C–O–O*. Subsequently, the reduction of the oxygen goes through the addition of 2 H^+ and 2 e^-, from the electrolyte and the electrode, respectively, forming -OOH that can be desorbed as H_2O_2. It has been reported that porosity plays a role in the reduction of the formed H_2O_2 in another active site, which could result in the reduction to water [47,48,50,51]. The calculated distance of the O–O atoms supports this mechanism. Initially the O=O molecule has a distance of 1.207 Å [52]; when the molecule is adsorbed and reduced the distance increases to a value close to the one for the hydrogen peroxide molecule (H_2O_2: $d_{O-O} = 1.490$ Å [52]).
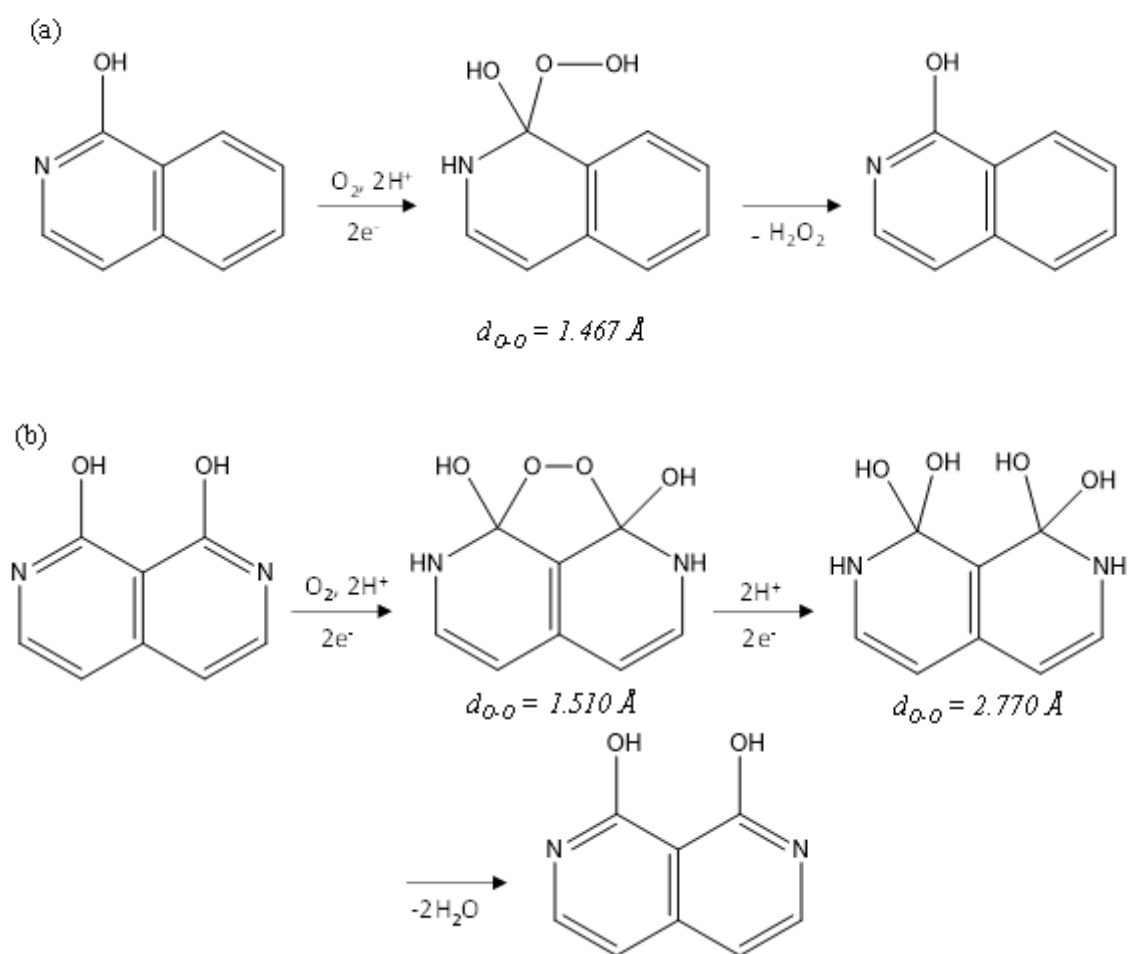

Fig. 10 Proposed pathway for ORR with (a) one active site and, (b) two active sites.

In the second mechanism (Fig. 10b), there are two active sites due to the presence of two adjacent N-C-O species. In this case, the adsorption of the dioxygen in the two active sites may form a bridge-like –C–O–O–C– configuration (step 2 in Fig. 10b). The breaking of the O–O bond leads to the formation of –OH groups and, subsequently, the formation of H_2O molecules without the formation of H_2O_2. The distance between the oxygen atoms confirms this possibility. In the bridge-like structure the O–O distance is slightly higher than in the case of the first mechanism although a value close to H_2O_2 is obtained. When the second 2 e^- step occurs and –OH are formed the calculated O–O distance is much higher (2.770 Å), which is close to the distance between the water molecules (H_2O-H_2O: d_{O-O} = 2.83 Å [53]), proving the dioxygen dissociation.

Thus, the presence of these sites may produce a change in ORR selectivity, being as close as 4e^- pathway with H_2O as final product, with increasing the number of double N-C-O sites. The experimental results show that the PANI carbon materials prepared in an O_2-containing atmosphere have a higher amount of N and O edge sites and, then, a higher probability of having the above mentioned sites, which explains the higher electron transfer number, being close to 4 in acidic conditions (Table 6).

4. CONCLUSIONS

N- and O-containing carbon materials have been prepared from PANI and evaluated as electrocatalysts for the ORR. The synthesis was performed using two different temperatures and atmospheres during the treatment, which leads to materials with different surface chemistry. Materials treated in inert atmosphere showed lower yields than the prepared using an O_2-containing atmosphere, which points out that the use of a slightly oxidant atmosphere promotes the crosslinking reactions and further condensation reactions during the carbonization. Slight differences in porosity are observed due to the low amount of O_2 used. The heat treatment at 800 ºC in an O_2-containing atmosphere generates, compared to the treatment in N_2, a higher amount of N-functionalities at edge sites (i.e., pyridine and pyridone/pyrrole groups) as well as an increase in phenol-type groups.

The prepared materials at 800 ºC in an O_2-containing atmosphere have a high electroactivity towards ORR in basic electrolyte with limiting specific currents close to the commercial sample 20% Pt/Vulcan. A detailed study of the effect of N and O functionalities confirm that a combination of N and O-containing groups at edge sites in the carbon material produced the highest ORR activity and higher selectivity to the 4e$^-$ pathway, especially in acid electrolyte. It is suggested that the presence of N-C-O species is the responsible for the enhanced ORR activity of the carbon materials prepared from PANI in the O_2-containing atmosphere.

These results are supported by preliminary computational calculations. It was observed that the N-C-O groups produce a much higher positive charge density in the C atom than the nitrogen groups without the presence of oxygen in the vicinities, which favors dioxygen adsorption and activation. It is proposed that one N-C-O site would mainly produce hydrogen peroxide through a 2e$^-$ pathway while the existence of two near sites (like two pyridones) can produce the direct reduction of dioxygen to water.

REFERENCES

[1]   Winter M, Brodd RJ. What Are Batteries, Fuel Cells, and Supercapacitors? Chem Rev. 2004;104(10):4245–70

[2]   Aricò AS, Bruce P, Scrosati B, Tarascon J-M, van Schalkwijk W. Nanostructured materials for advanced energy conversion and storage devices. Nat Mater. 2005;4(5):366–77

[3]   Bezerra CWB, Zhang L, Liu H, Lee K, Marques ALB, Marques EP, et al. A review of heat-treatment effects on activity and stability of PEM fuel cell catalysts for oxygen reduction reaction. J Power Sources. 2007;173(2):891–908

[4]   Zhao X, Chen S, Fang Z, Ding J, Sang W, Wang Y, et al. Octahedral Pd@Pt $_{1.8}$ Ni Core–
        Shell Nanocrystals with Ultrathin PtNi Alloy Shells as Active Catalysts for Oxygen
        Reduction Reaction. J Am Chem Soc. 2015;137(8):2804–7

[5]   Yu X, Ye S. Recent advances in activity and durability enhancement of Pt/C catalytic
        cathode in PEMFC. J Power Sources. 2007;172(1):133–44

[6]   Xu B, Yang X, Wang X, Guo J, Liu X. A novel catalyst support for DMFC: Onion-like
        fullerenes. J Power Sources. 2006;162(1):160–4

[7]   Zaragoza-Martín F, Sopeña-Escario D, Morallón E, de Lecea CS-M. Pt/carbon
        nanofibers electrocatalysts for fuel cells. J Power Sources. 2007;171(2):302–9

[8]   Morozan A, Jousselme B, Palacin S. Low-platinum and platinum-free catalysts for the
        oxygen reduction reaction at fuel cell cathodes. Energy Environ Sci. 2011;4(4):1238–54

[9]   Zhang L, Zhang J, Wilkinson DP, Wang H. Progress in preparation of non-noble
        electrocatalysts for PEM fuel cell reactions. J Power Sources. 2006;156(2):171–82

[10]   Jaouen F, Proietti E, Lefèvre M, Chenitz R, Dodelet J-P, Wu G, et al. Recent advances in
        non-precious metal catalysis for oxygen-reduction reaction in polymer electrolyte
        fuelcells. Energy Environ Sci. 2011;4(1):114–30

[11]   Ozaki J, Tanifuji S, Furuichi A, Yabutsuka K. Enhancement of oxygen reduction activity
        of nanoshell carbons by introducing nitrogen atoms from metal phthalocyanines.
        Electrochim Acta. 2010;55(6):1864–71

[12]   Rao CV, Cabrera CR, Ishikawa Y. In Search of the Active Site in Nitrogen-Doped
        Carbon Nanotube Electrodes for the Oxygen Reduction Reaction. J Phys Chem Lett.
        2010;1(18):2622–7

[13]   Shen W, Fan W. Nitrogen-containing porous carbons: synthesis and application. J Mater
        Chem A. 2013;1(4):999–1013

[14]   Strelko VV, Kuts VS, Thrower PA. On the mechanism of possible influence of

heteroatoms of nitrogen, boron and phosphorus in a carbon matrix on the catalytic activity of carbons in electron transfer reactions. Carbon. 2000;38(10):1499–503

[15] Strelko VV, Kartel NT, Dukhno IN, Kuts VS, Clarkson RB, Odintsov BM. Mechanism of reductive oxygen adsorption on active carbons with various surface chemistry. Surf Sci. 2004;548(1–3):281–90

[16] Maldonado S, Stevenson KJ. Influence of Nitrogen Doping on Oxygen Reduction Electrocatalysis at Carbon Nanofiber Electrodes. J Phys Chem B. 2005;109(10):4707–16

[17] Gong K, Du F, Xia Z, Durstock M, Dai L. Nitrogen-Doped Carbon Nanotube Arrays with High Electrocatalytic Activity for Oxygen Reduction. Science. 2009;323(5915):760–4

[18] Wiggins-Camacho JD, Stevenson KJ. Mechanistic Discussion of the Oxygen Reduction Reaction at Nitrogen-Doped Carbon Nanotubes. J Phys Chem C. 2011;115(40):20002–10

[19] Mostazo-López MJ, Ruiz-Rosas R, Morallón E, Cazorla-Amorós D. Generation of nitrogen functionalities on activated carbons by amidation reactions and Hofmann rearrangement: Chemical and electrochemical characterization. Carbon. 2015;91:252–65

[20] Raymundo-Piñero E, Cazorla-Amorós D, Linares-Solano A. The role of different nitrogen functional groups on the removal of SO2 from flue gases by N-doped activated carbon powders and fibres. Carbon. 2003;41(10):1925–32

[21] Raymundo-Pinero E, Cazorla-Amorós D, Linares-Solano A, Delpeux S, Frackowiak E, Szostak K, et al. High surface area carbon nanotubes prepared by chemical activation. Carbon. 2002;40:1614–7

[22] Salinas-Torres D, Sieben JM, Lozano-Castello D, Morallón E, Burghammer M, Riekel C, et al. Characterization of activated carbon fiber/polyaniline materials by position-resolved microbeam small-angle X-ray scattering. Carbon. 2012;50(3):1051–6

[23]   Singh KP, Song MY, Yu J-S. Iodine-treated heteroatom-doped carbon: conductivity driven electrocatalytic activity. J Mater Chem A. 2014;2(42):18115–24

[24]   Ćirić-Marjanović G, Pašti I, Gavrilov N, Janošević A, Mentus S. Carbonised polyaniline and polypyrrole: towards advanced nitrogen-containing carbon materials. Chem Pap. 2013;67(8):781–813

[25]   Cazorla-Amorós D, Alcañiz-Monge J, de la Casa-Lillo MA, Linares-Solano A. CO2 As an Adsorptive To Characterize Carbon Molecular Sieves and Activated Carbons. Langmuir. 1998;7463(14):4589–96

[26]   Hanwell MD, Curtis DE, Lonie DC, Vandermeerschd T, Zurek E, Hutchison GR. Avogadro: An advanced semantic chemical editor, visualization, and analysis platform. J Cheminform. 2012;4(8):17

[27]   Frisch MJ, Trucks GW, Schlegel HB, Scuseria GE, Robb MA, Cheeseman JR, et al. Gaussian 09, Revision B.01, Gaussian, Inc., Wallingford CT; 2009.

[28]   Alcañiz-Monge J, Cazorla-Amorós D, Linares-Solano A, Oya A, Sakamoto A, Hoshi K. Preparation of general purpose carbon fibers from coal tar pitches with low softening point. Carbon. 1997;35(97)

[29]   Biniak S, Szymański G, Siedlewski J, ŚwiąTkowski a. The characterization of activated carbons with oxygen and nitrogen surface groups. Carbon. 1997;35(12):1799–810

[30]   Raymundo-Piñero E, Cazorla-Amorós D, Linares-Solano A, Find J, Wild U, Schlögl R. Structural characterization of N-containing activated carbon fibers prepared from a low softening point petroleum pitch and a melamine resin. Carbon. 2002;40(4):597–608

[31]   Salinas-Torres D, Shiraishi S, Morallón E, Cazorla-Amorós D. Improvement of carbon materials performance by nitrogen functional groups in electrochemical capacitors in organic electrolyte at severe conditions. Carbon. 2015;82:205–13

[32]   Kuroki S, Hosaka Y, Yamauchi C. A solid-state NMR study of the carbonization of

polyaniline. Carbon. 2013;55:160–7

[33]   Rozlívková Z, Trchová M, Exnerová M, Stejskal J. The carbonization of granular

       polyaniline to produce nitrogen-containing carbon. Synth Met. 2011;161(11):1122–9

[34]   Figueiredo JL, Pereira MFR, Freitas MMA, Orfao JJM. Modification of the surface

       chemistry of activated carbons. Carbon. 1999;37(9):1379–89

[35]   Otake Y, Jenkins RG. Characterization of oxygen-containing surface complexes created

       on a microporous carbon by air and nitric acid treatment. Carbon. 1993;31(1):109–21

[36]   Román-Martínez MCC, Cazorla-Amorós D, Linares-Solano A, de Lecea CS-M. TPD

       and TPR characterization of carbonaceous supports and Pt/C catalysts. Carbon.

       1993;31(6):895–902

[37]   Burg P, Cagniant D. Characterization of Carbon Surface Chemistry. In: Radovic LR,

       editor. Chemistry & Physics of Carbon. Vol. 30. Taylor & Francis (CRC Press); 2008. p.

       129–75

[38]   Berenguer R, Marco-Lozar JP, Quijada C, Cazorla-Amorós D, Morallón E. Effect of

       electrochemical treatments on the surface chemistry of activated carbon. Carbon.

       2009;47(4):1018–27

[39]   Gorgulho HF, Mesquita JP, Gonçalves F, Pereira MFR, Figueiredo JL. Characterization

       of the surface chemistry of carbon materials by potentiometric titrations and

       temperature-programmed desorption. Carbon. 2008;46(12):1544–55

[40]   Ornelas O, Sieben JM, Ruiz-Rosas R, Morallón E, Cazorla-Amorós D, Geng J, et al. On

       the origin of the high capacitance of nitrogen-containing carbon nanotubes in acidic and

       alkaline electrolytes. Chem Commun. 2014;50(77):11343–6

[41]   Hulicova D, Yamashita J, Soneda Y, Hatori H, Kodama M. Supercapacitors Prepared

       from Melamine-Based Carbon. Chem Mater. 2005;17(5):1241–7

[42]   Hulicova-Jurcakova D, Kodama M, Shiraishi S, Hatori H, Zhu ZH, Lu GQ. Nitrogen-

Enriched Nonporous Carbon Electrodes with Extraordinary Supercapacitance. Adv Funct Mater. 2009;19(11):1800–9

[43]   Zhang L, Xia Z. Mechanisms of Oxygen Reduction Reaction on Nitrogen-Doped Graphene for Fuel Cells. J Phys Chem C. 2011;115(22):11170-6

[44]   Kim H, Lee K, Woo SI, Jung Y, Sheng W, Gasteiger HA, et al. On the mechanism of enhanced oxygen reduction reaction in nitrogen-doped graphene nanoribbons. Phys Chem Chem Phys. 2011;13(39):17505

[45]   Silva R, Voiry D, Chhowalla M, Asefa T. Efficient Metal-Free Electrocatalysts for Oxygen Reduction: Polyaniline-Derived N- and O-Doped Mesoporous Carbons. J Am Chem Soc. 2013;135:7823–6

[46]   Ozaki J, Kimura N, Anahara T, Oya A. Preparation and oxygen reduction activity of BN-doped carbons. Carbon. 2007;45(9):1847–53

[47]   Park J, Nabae Y, Hayakawa T, Kakimoto M. Highly Selective Two-Electron Oxygen Reduction Catalyzed by Mesoporous Nitrogen-Doped Carbon. ACS Catal. 2014;4(10):3749–54

[48]   Domínguez C, Pérez-Alonso FJ, Abdel Salam M, Al-Thabaiti SA, Obaid AY, Alshehri AA, et al. On the relationship between N content, textural properties and catalytic performance for the oxygen reduction reaction of N/CNT. Appl Catal B Environ. 2015;162:420–9

[49]   Ikeda T, Boero M, Huang S-F, Terakura K, Oshima M, Ozaki J. Carbon Alloy Catalysts: Active Sites for Oxygen Reduction Reaction. J Phys Chem C. 2008;112(38):14706–9

[50]   Wong WY, Daud WRW, Mohamad AB, Kadhum AAH, Loh KS, Majlan EH, et al. The Impact of Loading and Temperature on the Oxygen Reduction Reaction at Nitrogen-doped Carbon Nanotubes in Alkaline Medium. Electrochim Acta. 2014;129:47–54

[51]   Seredych M, Szczurek A, Fierro V, Celzard A, Bandosz TJ. Electrochemical Reduction

of Oxygen on Hydrophobic Ultramicroporous PolyHIPE Carbon. ACS Catal. 2016;6(8):5618–28

[52]   Greenwood NN, Earnshaw A. Chemistry of the Elements. 2nd ed. Elsevier Butterworth-Heinemann; 1997. 1342 p.

[53]   Clementi E. Determination of Liquid Water Structure. In: Carpenter B, Ceroni P, Kirchner B, Landfester K, Leszczynski J, Luh T-Y, et al., editors. Lecture Notes in Chemistry vol 2. 1st ed. Berlin, Heidelberg: Springer; 1976.

Supplementary Material